

Spin Dependence in the Deuteron Optical Model

W. HAEBERLI

University of Wisconsin, Madison

1. Introduction

Over the last ten years many experiments have been reported which studied the interaction between deuterons and nuclei. It has been shown that the differential cross section, $\sigma(\theta)$, for deuteron elastic scattering in many cases can be described with considerable accuracy by an optical model similar to that used to describe scattering of protons and neutrons. Hodgson¹ summarized the available information on the deuteron optical model five years ago in an excellent review paper. It was found that the observations generally are consistent with the idea that the potential for the deuteron should be related to the nucleon potential. In the most naive picture, we might think of a deuteron potential simply as the sum of the neutron and proton potential. The nucleon potentials are to be taken at an energy equal to one-half the deuteron energy. Since the well-depth for nucleon scattering is roughly 50 MeV, this leads to a central potential for deuterons of about 100 MeV. While the experimental cross sections can be described with several discrete values of the deuteron well depth (e.g. 50 MeV, 100 MeV, 150 MeV), the above argument leads one to prefer the 100 MeV deep potential. This conclusion remains unchanged if one treats the problem in a more sophisticated way, i.e., if one averages the neutron and proton potential over the wave function of the deuteron, as proposed by Watanabe² and others. In this model, the large size of the deuteron leads to a potential well which falls off less rapidly than that for nucleons. Testoni and Gomes³, for instance, find a diffuseness parameter of 0.85 fm for the deuteron potential, as opposed to 0.65 fm for the nucleon potential. The imaginary part of the deuteron potential cannot readily be obtained from these arguments because the deuteron is subject to break-up which has no counterpart in nucleon scattering.

The deuteron potential commonly used to analyze deuteron elastic cross sections consists of the Coulomb potential $V_c(r)$, a central potential of depth U (~ 100 MeV) and radial dependence $f(r)$ of the Woods-Saxon

type, and an absorptive potential of strength W and radial dependence $g(r)$ peaked near the nuclear surface (derivative of Woods-Saxon form):

$$V(\text{central}) = V_c(r) + U f(r) + iW g(r).$$

This type of potential neglects the fact that the deuteron has spin. We know that in nuclei the spin-orbit force is strong. The magnitude of the spin-orbit potential between nucleons and nuclei is roughly 6 MeV^4 . The primary purpose of this paper is to report on experiments to investigate the spin-dependence for the deuteron-nucleus interaction.

2. Scattering of Polarized Deuterons

The most straightforward way to study the spin-dependence is to perform scattering experiments with a polarized beam. If the beam polarization is turned on, the scattering cross section changes. The fractional change in the cross section divided by the change in beam polarization is called the analyzing power of the reaction. The larger the analyzing power, the larger is the degree of spin-dependence of the scattering process. For scattering of spin-1/2 particles, only one analyzing power is needed to describe the scattering. For deuterons, the situation is more complicated because we are dealing with particles of spin one (see Ref. 5). The cross section expression for the scattering of polarized deuterons⁵ involves four analyzing powers, namely a vector analyzing power iT_{11} and three tensor analyzing powers T_{20} , T_{21} and T_{22} . To measure these quantities we must use a polarized beam with vector polarization t_v , and/or tensor polarizations t_{20} , t_{21} and t_{22} . If one wishes to measure iT_{11} , one prefers to use a beam with zero tensor polarization. This can be done by suitable operation of a polarized-ion source^{6,7}. The vector polarization of the beam causes a $\cos\phi$ -dependence (left-right asymmetry) in the cross section just as in the case of proton scattering. To measure the tensor polarization parameters we can operate the ion source (see Ref. 6) to produce the same number of deuterons in the $m_I = +1$ state as in the $m_I = -1$ state, but a different number (ideally all or none) in the $m_I = 0$ state (aligned beam, no vector polarization). By use of spin-precession devices between the ion source and the accelerator we can choose the alignment axis of the beam in any desired direction with respect to the beam direction and the normal to the scattering plane.

Suppose the alignment axis $\mathbf{3}$ makes an angle α with the incident beam direction and is rotated by an angle ϕ about the beam axis where we choose $\phi = 0$ to be in a plane perpendicular to the scattering plane (Fig. 1). The

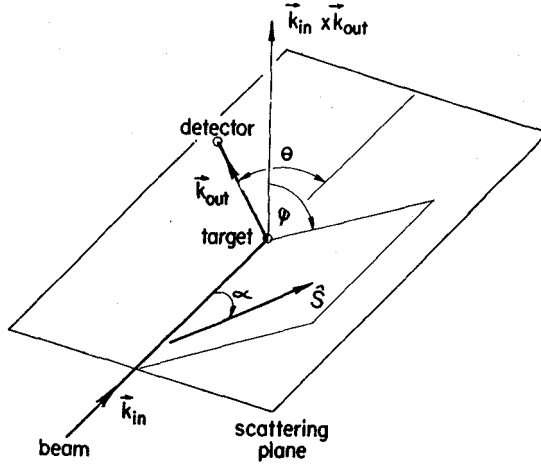


Fig. 1 - Diagram illustrating the vector quantities important in the scattering of polarized beams.

expression for the cross section will now contain terms containing the tensor analyzing powers. The T_{22} analyzing power is characterized by a **cos 2ϕ -dependence** in the cross section, T_{21} causes a **sin ϕ -dependence**, while T_{20} causes a change in the cross section which is independent of ϕ . The expression for the cross section for a pure **tensor-polarized** beam (i.e., same number in the $m_s = +1$ and $m_t = -1$ states) is given by (eq. 26 of Ref. 5)

$$\sigma(\theta, \phi) = \sigma(\theta) \left[1 + \frac{1}{2} \tau (3 \cos^2 \alpha - 1) T_{20} - \sqrt{\frac{3}{2}} \tau \sin 2\alpha \sin \phi T_{21} - \sqrt{\frac{3}{2}} \tau \sin^2 \alpha \cos \phi T_{22} \right],$$

where $\tau = \frac{1}{\sqrt{2}}(1 - 3N_0)$ is a measure of the alignment of the **beam**. We can separately determine the (unpolarized) differential cross section $\sigma(\theta)$ and **all** three tensor analyzing powers if we measure the cross section with four different sets of alignment directions (a, 4) **since** this will give us four equations with four unknowns. In practice, we have **used** a slightly **different** method. We measure $\sigma(\theta)$ by turning off the source-polarization ($t = 0$) and take three measurements with the **polarized** beam, one for $a = 0$ (alignment along the beam), one for $\alpha = 90^\circ, \phi = 0^\circ$ (alignment up) and a third one for $a = 45^\circ, \phi = 90^\circ$ (alignment in the scattering plane). The first of these ($a = 0$) measures T_{20} independently of T_{21} and T_{22} . The second measurement gives us a maximum sensitivity to T_{22} , the third a

maximum sensitivity to T_{21} . The set of measurements given above is for illustration only. Other orientations of the alignment axis could be chosen. It is possible, for instance, to choose the alignment axis such that only one of the three beam tensor parameters is different from zero. In part, the choice is influenced by error considerations: one wishes to choose conditions which produce large changes in the beam tensor moments from one orientation to the next and conditions for which a small error in the orientation has little effect on the measurements.

The polarized-beam current on target for our experiments is typically 10-20 nA. After passing through the target chamber, the unscattered beam enters a second chamber where the beam polarization is monitored continuously during the experiment. In this way, any malfunctioning of the polarized-ion source or any error in the spin-precession angles is detected immediately. The scattered deuterons are simultaneously detected at four scattering angles by means of four counter telescopes consisting each of a 100 μm thick ΔE -detector and a 2.5 mm thick E-detector. Scattered deuterons are distinguished from (d,p)-protons by on-line analysis of the pulses in a computer.

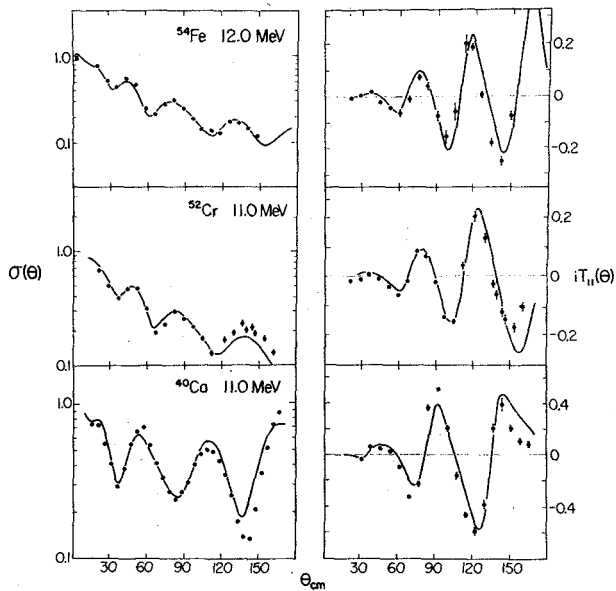


Fig. 2 - Differential cross sections and vector analysing powers for elastic deuteron scattering on ^{54}Fe , ^{52}Cr and ^{40}Ca .

3. Measurements of the **Vector** Analyzing Power

A few examples of recent measurements of the vector analyzing powers are shown in Figs. 2 and 3 for targets between ^{40}Ca and ^{208}Pb . These measurements were obtained by Schwandt, Bjorkholm, Kocher and Rathmell at our laboratory. The analyzing power is large for ^{40}Ca and decreases with increasing atomic weight of the target. For ^{208}Pb , where the bombarding energy is near the Coulomb barrier, the effects become quite small but are still easily detected. Additional measurements were made recently by Lohr for many targets at deuteron energies of 9, 11 and 13 MeV. One example is shown in Fig. 4. The analyzing power is seen to increase rapidly with deuteron energy. The angular dependence of iT_{11} shows period oscillations which are related to the oscillations in the cross section. It is found that the position of the maxima and minima of iT_{11} depends in a systematic way on the nuclear radius, indicating that analysis in terms of a potential

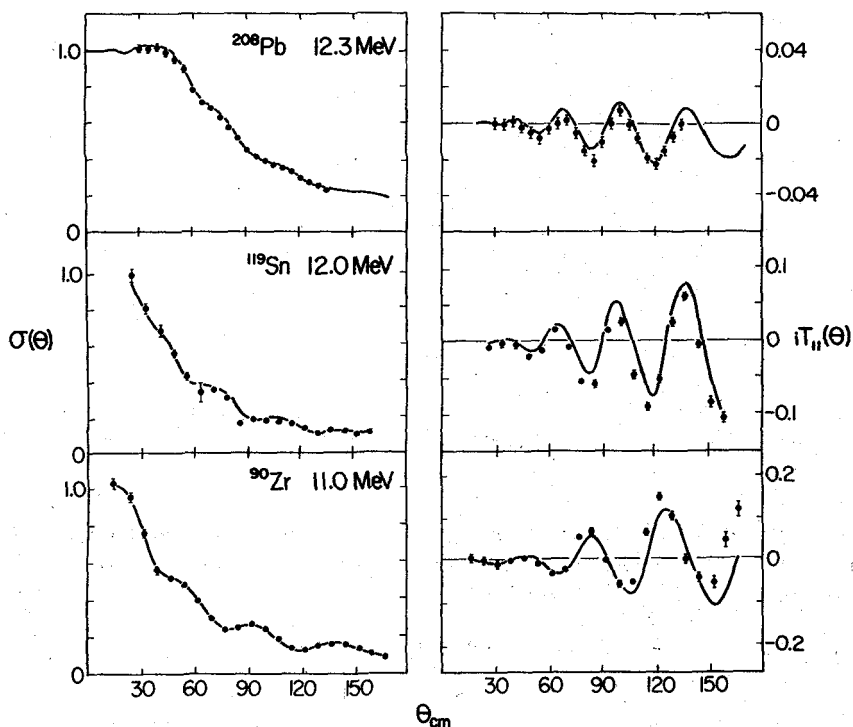


Fig. 3 - Differential cross sections and vector analyzing powers for elastic deuteron scattering on ^{208}Pb , ^{119}Sn and ^{90}Zr .

model is meaningful. The energy dependence has been studied most extensively for ^{40}Ca , where measurements between 5 and 11 MeV are available from Wisconsin⁸ and results at 21.4 MeV from Saclay⁹ (Fig. 5). The magnitude and complexity of $iT_{11}(\theta)$ increases considerably from 7 to 21.4 MeV.

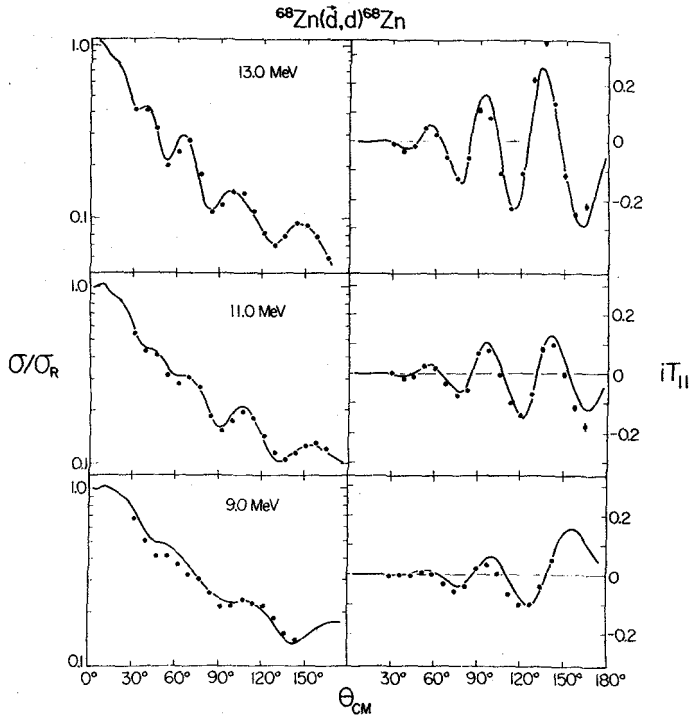


Fig. 4 - The differential cross sections and vector analysing powers for elastic deuteron scattering on ^{68}Zn for three different bombarding energies.

The curves shown in the above figures are based on optical model calculations. The potential consists of a central potential to which a spin-orbit term of the form $L \cdot S$ is added:

$$V = V(\text{central}) + V(L \cdot S).$$

The radial dependence of $V(L \cdot S)$ is of the Thomas form. The model reproduces the main features of the measurements reasonably well. The general conclusion is that the radius and diffuseness of the spin-orbit potential are both about 20% smaller than the corresponding parameters

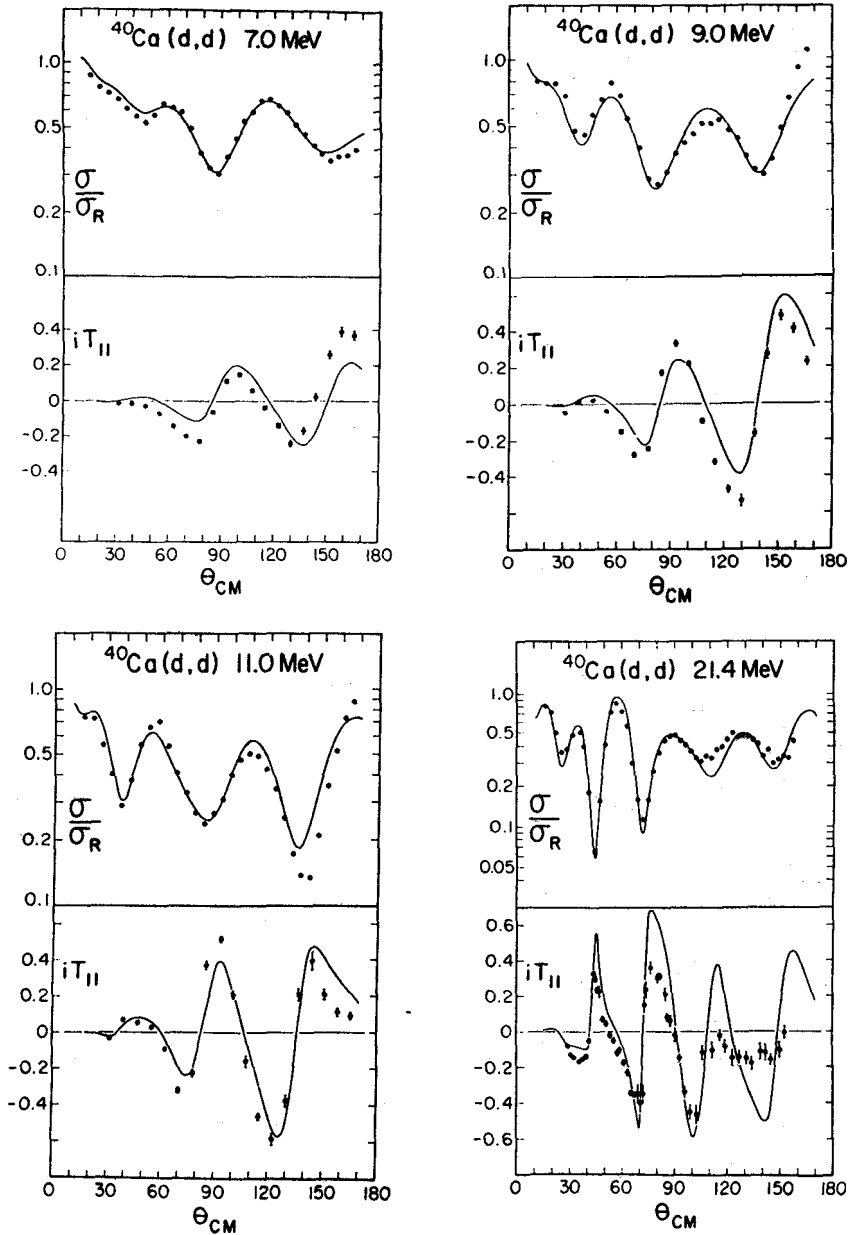


Fig. 5 - Energy dependence of the differential cross sections and vector analysing powers for elastic deuteron scattering on ^{40}Ca .

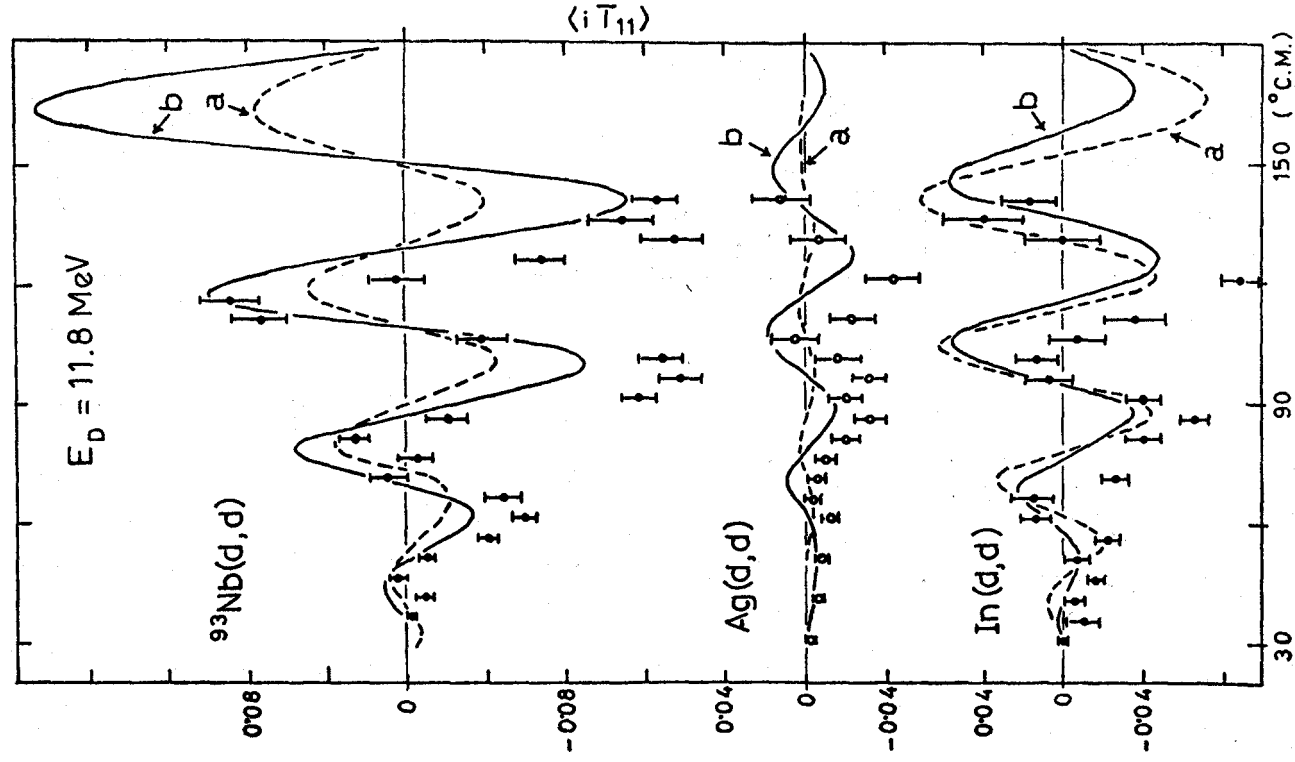


Fig. 6 - Vector analysing power for the elastic scattering of deuterons by ^{93}Nb , Ag and In . The curves represent optical-model calculations. The figure is from Ref. 11.

of the central potential. The strength of the spin-orbit term is about 6 MeV and of the same sign as for nucleon scattering. The strength is compatible¹⁰ with the idea that the spin-orbit force arises from the nucleon spin-orbit force, taking into account that the deuteron is in a triplet state and each nucleon in the deuteron carries one-half the deuteron orbital angular momentum.

In all our work we assumed a depth of the central potential near $V = 100$ MeV. The question arises whether polarization data can be used to eliminate the ambiguity in V . Fig. 6 shows results by the Birmingham group¹¹ where the dashed curves are for $V \sim 60$ MeV, the solid curves for $V \sim 110$ MeV. While the deeper potential gives a better fit, it is not clear whether suitable adjustments of the parameters for the shallower potential could not give satisfactory agreement also. In particular the amplitude of oscillations for ^{93}Nb could presumably be increased by using a larger spin-orbit strength. More work along this line should be done since in the analysis of the 21.4 MeV data on ^{40}Ca Raynal¹² also finds a strong preference for the deeper potential.

In all analyses of this kind the spin of the target nucleus is neglected entirely. A comparison between scattering from ^{52}Cr and ^{53}Cr (spin 3/2) shows that there is no difference which could be attributed to the target spin (Fig. 7).

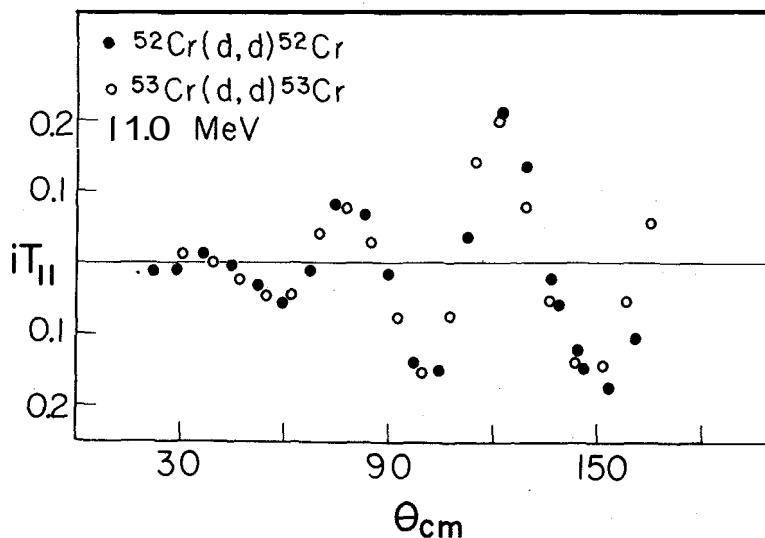


Fig. 7 - Vector analysing powers for the elastic scattering of deuterons by ^{52}Cr and ^{53}Cr .

4. Measurements of the Tensor Analyzing Powers

The first measurements of tensor analyzing powers were done at Saclay⁹ and Wisconsin¹³. Only two of the three moments were measured (T_{20} and T_{22}) since facilities were lacking for flexible spin precession. Obviously, measurements of the tensor moments are of interest because they provide much more experimental information than the cross section and vector analyzing power. In particular, these measurements are important to determine whether tensor forces act between the deuteron and the nucleus, in addition to the $\mathbf{L} \cdot \mathbf{S}$ force. In order to construct a tensor potential, Satchler¹⁴ considered interactions which depend on deuteron spin S , position r , momentum p and angular momentum L . He showed that parity conservation and symmetry of the scattering matrix limits the forms of the tensor potential to three types which we will label T_{SR} , T_{LS} and T_{SP} :

$$\begin{aligned} T_{SR}(r) &= \frac{(\mathbf{S} \cdot \mathbf{r})^2}{r^2} - \frac{2}{3}, \\ T_{LS}(r) &= (\mathbf{L} \cdot \mathbf{S})^2 + \frac{1}{2}(\mathbf{L} \cdot \mathbf{S}) + 2L^2, \\ T_{SP}(r) &= (\mathbf{S} \cdot \mathbf{p})^2 - \frac{2}{3}p^2. \end{aligned}$$

Each of the above terms is to be multiplied by a corresponding potential depth and a function describing the radial dependence.

It has been shown¹⁵ that the tensor interaction is expected to have relatively little effect on the vector analyzing powers, but enters strongly into the tensor analyzing powers. More specifically, if we express the interaction as

$$V = V(\text{central}) + V(\mathbf{L} \cdot \mathbf{S}) + V(\text{tensor}),$$

and assume the spin-dependent potentials to be weak compared to the central potential, the vector analyzing power depends on first-order terms in $V(\mathbf{L} \cdot \mathbf{S})$, while the tensor analyzing powers involve terms of second order in $V(\mathbf{L} \cdot \mathbf{S})$, but first order terms in $V(\text{tensor})$ (see Ref. 15).

Raynal¹² analyzed the Saclay tensor measurements for ^{40}Ca and concluded that there was no evidence for tensor interaction. The first evidence for a tensor interaction was presented by Schwandt and Haeberli^{8,13} who analyzed a , iT_{11} , T_{20} and T_{22} for deuteron scattering from Al and ^{40}Ca . Fig. 8 shows that indeed a tensor potential of the type T_{SR} improves the fit to the measured T_{20} and T_{22} . The same was found for scattering from Al . In both cases the $\mathbf{S} \cdot \mathbf{r}$ interaction was attractive ($V_{SR} \approx 5 \text{ MeV}$) and of long range ($r_c = 1.4 \text{ fm}$). A slight improvement is

$^{40}\text{Ca}(d,d), 21.4\text{ MeV}$

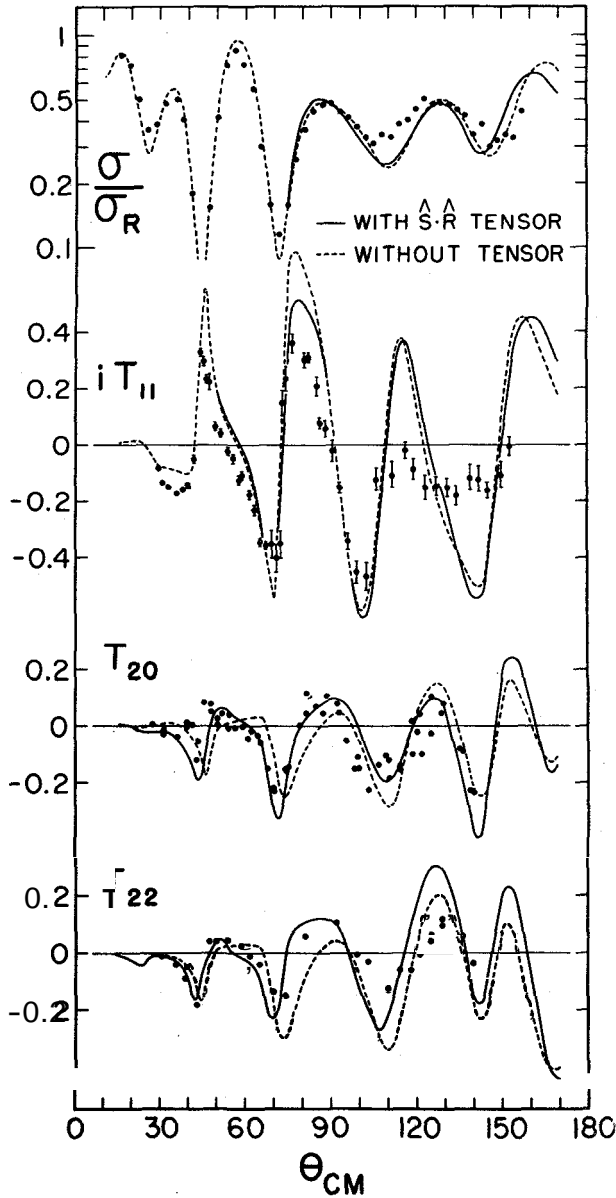


Fig. 8 - Differential cross section, and vector and tensor analysing powers for elastic scattering of deuterons by ^{40}Ca at 21.4 MeV. The figure is from Ref. 8.

also noted for the ^{40}Ca measurements at 9 MeV (Fig. 9) but a tensor potential of form T_{LS} has an adverse effect on iT_{11} . The evidence for a T_{SR} potential is still marginal but it is very interesting to note¹⁶ that the sign and strength of the potential which we found by straightforward data fitting agrees quantitatively with the T_{SR} potential predicted by Raynal¹⁷ on the basis of the Watanabe model. The T_{SR} term in this case arises from the D-state of the deuteron^{3,14,16}. In the same model, potentials of the form T_{SP} and T_{LS} can arise from the non-locality of the nucleon optical potentials¹⁵.

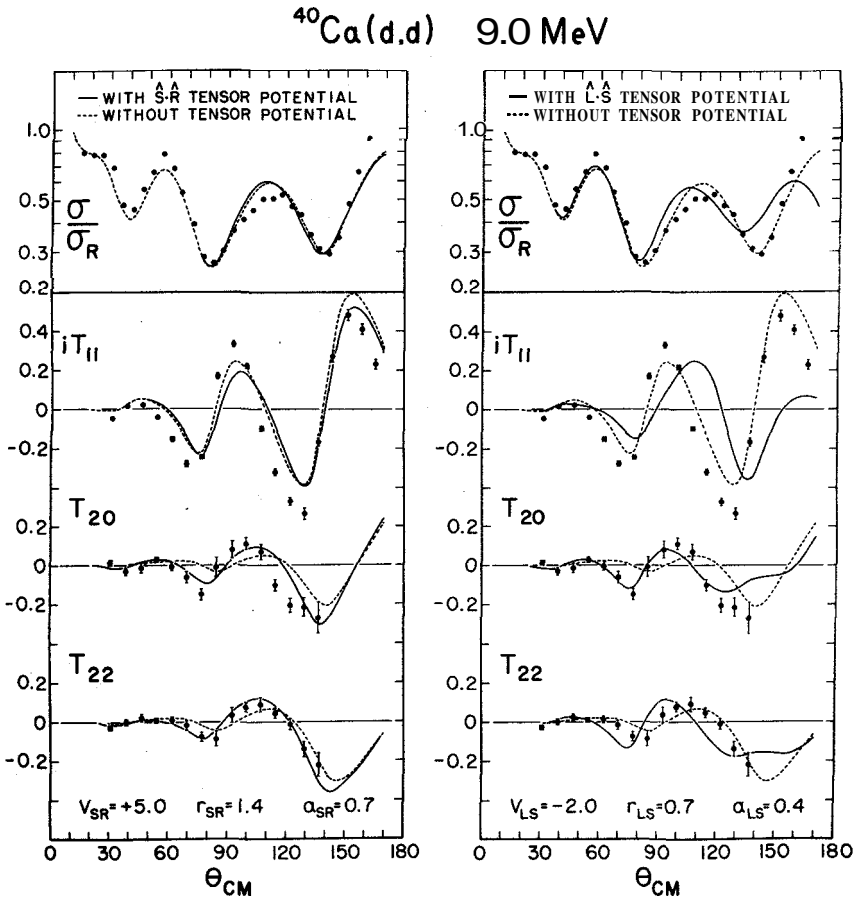


Fig. 9 - Differential cross section, and vector and tensor analysing powers for elastic scattering of deuterons by ^{40}Ca at 9 MeV. The figure is from Ref. 8.

$^{28}\text{Si} (d,d) ^{28}\text{Si} \quad 7.0 \text{ MeV}$

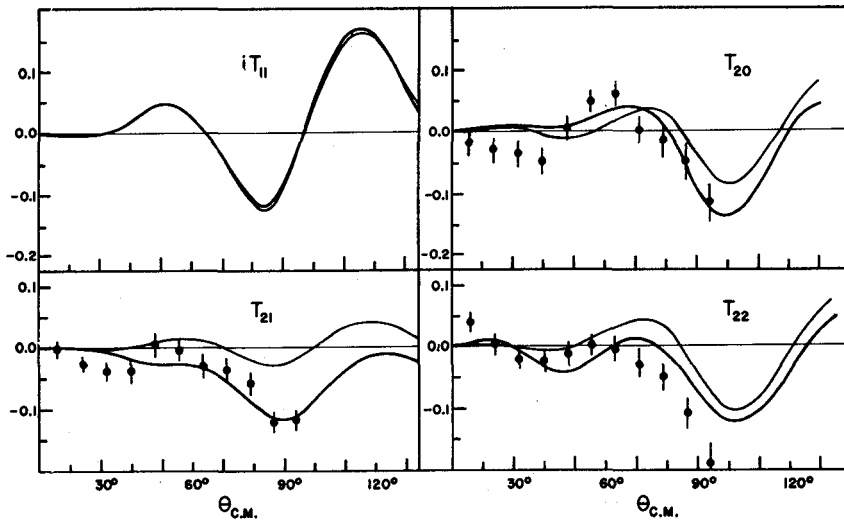


Fig. 10 - Tensor and vector analyzing powers for the elastic scattering of deuterons by ^{28}Si . The curves are explained in the text. The figure is from Ref. 18.

Additional evidence for a tensor potential arises from the recent Canberra measurements¹⁸ of all three tensor moments in deuteron scattering from ^{24}Mg and ^{28}Si . Their results for ^{28}Si at 7 MeV are shown in Fig. 10. The light curves are calculated with a spin-orbit force only, the heavy lines with spin-orbit force and T_{SR} tensor potential. The most interesting feature is that T_{21} , which was not determined in the earlier experiments, seems to be the quantity most sensitive to tensor interaction. It would seem extremely useful to have measurements of all three tensor analyzing powers for heavier nuclei. Goddard at our laboratory has started such experiments. As an example, measurements on ^{54}Fe at 10 MeV are shown in Fig. 11. The solid curves are predictions based on $V(\text{central}) + V(\mathbf{L} \cdot \mathbf{S})$, where the potential parameters were determined by fitting cross sections and vector analyzing powers. The agreement is poor but again we note in particular that the predicted T_{21} is much too small. A tensor term of the type (T_{SR}) and magnitude proposed by Schwandt⁵ gives more reasonable magnitudes of T_{21} (dashed curve) but no agreement with the data. Much work will still be required on this problem.

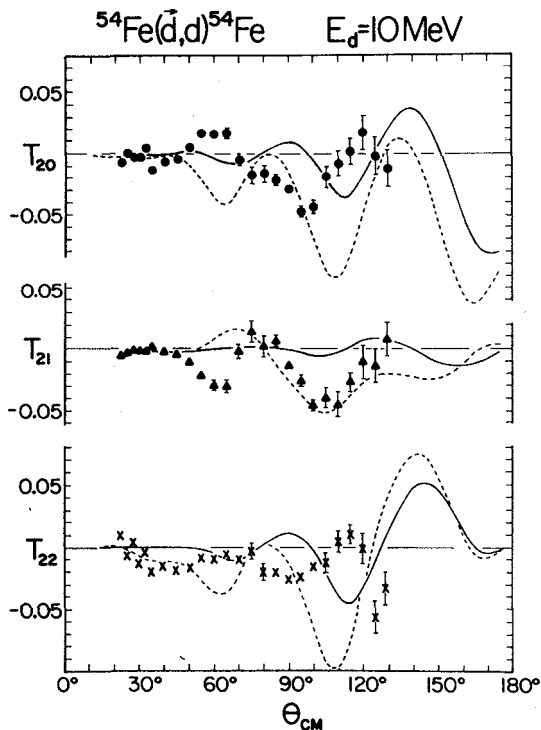


Fig. 11 - Tensor analysing powers for the elastic scattering of deuterons by ^{54}Fe .

5. Tensor Effects in the Coulomb Interaction

L. Knutson at our laboratory has recently done an experiment to investigate the tensor interaction which occurs in Coulomb scattering. From classical electrostatics we know that the force on a deuteron in an electric field should consist of a part equal to the deuteron charge times the electric field, plus a part which is proportional to the deuteron electric quadrupole moment times the second derivative of the electric field. The second part depends on the orientation of the deuteron and leads to a tensor interaction, as first pointed out by Raynal¹⁶. The effective potential which arises from the deuteron quadrupole moment Q is

$$V_Q(r) = + \frac{3}{2} Q Z e^2 \frac{1}{r^3} T_{SR},$$

where T_{SR} is the same as before. Knutson made calculations of the expected analyzing powers for scattering of 9 MeV deuterons on lead. The results of the calculations are shown in Fig. 12. In order to estimate the effect of the nuclear potential, calculations were also made for $V(\text{central}) + V(\text{L.S.})$ using the parameters determined from deuteron scattering on ^{208}Pb at 12 MeV. The nuclear potential has a noticeable effect on the cross section (Fig. 12) but produces analyzing powers < 0.001 , i.e., there is not enough penetration into the nucleus to feel the spin-orbit force. Indeed the calculated iT_{11} are zero. The measured tensor analyzing powers are small as predicted by the calculations, but not in quantitative agreement with the predictions (Fig. 12). The results illustrate that very small polarization effects are now accessible to experiment. The fact that the measured iT_{11} is significantly different from zero may indicate that the spin-orbit term extends to larger radii than had been assumed. This, however, would not explain why the tensor analyzing powers are as large or larger than iT_{11} since the spin-orbit term is a second-order effect in the tensor analyzing powers¹⁵. Thus one may also need a weak long-range tensor interaction in addition to the quadrupole interaction. One objection to the calculations is that electric polarization of the deuteron and coupling to the stripping channels was neglected.

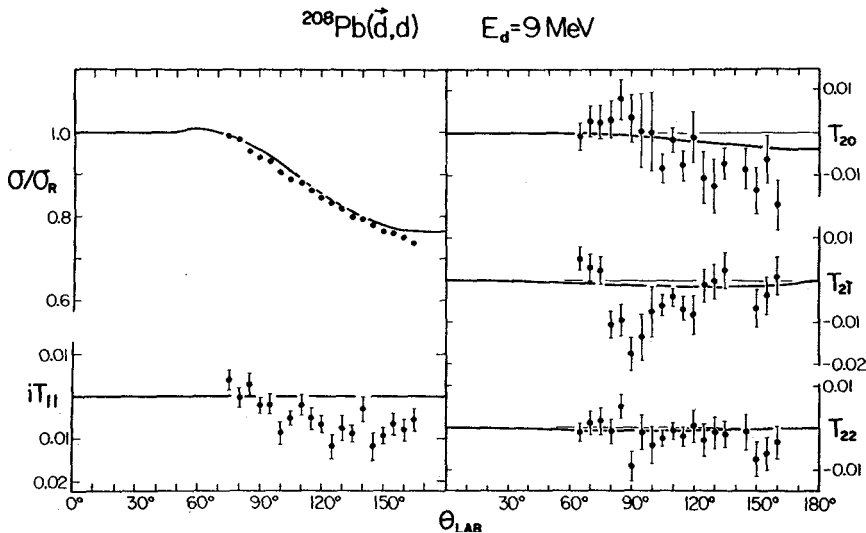


Fig. 12 - Differential cross section, and vector and tensor analyzing powers for the elastic scattering of deuterons by ^{208}Pb .

6. Nuclear Reactions Induced by Deuterons

Deuteron stripping reactions have been described very successfully by the distorted-wave theory (DWBA). The deuteron potential enters in the calculations as the distorting potential of the incoming deuteron wave. In contrast to elastic scattering, which is sensitive only to the **asymptotic form** of the deuteron wave function, the reaction will depend on the **deuteron** wave function near the nuclear surface and may be even inside the nucleus.

As a whole, cross sections calculated with DWBA are in reasonable agreement with experiment. One of the shortcomings of the calculations has been the **difficulty** of reproducing the behavior at large reaction angles. This is not particularly **surprising**, since at large angles the cross section is very small and thus very sensitive to small errors in the reaction **matrix** elements. The special **interest** in large reaction angles arises from the empirical observation by Lee and **Schiffer**^{19,20} that for large angles the cross section for $l = 1$ transitions shows a j -dependence, e.g. for $^{54}\text{Fe}(d, p)^{55}\text{Fe}$ the $j = 1/2^-$ transitions show a pronounced minimum in the cross section near 135° while the $j = 3/2^-$ transitions do not. Attempts to **explain** this feature by DWBA calculations were **unsuccessful**^{20,21} even though **adjustment** of various parameters (including the deuteron spin-orbit strength) were tried. It is interesting to note that the Lee-Schiffer effect is reproduced qualitatively without further adjustment of parameters when one uses deuteron potentials which are derived from measurements of the deuteron cross section and the vector analyzing power. An example is illustrated in Fig. 13 where on the left are shown curves through the experimental cross section **points**²⁰ and on the right the DWBA predictions. The agreement is by no means perfect, but the calculations **seem** to reproduce the **qualitative** features of the j -dependence, including the observation that at 8 MeV bombarding energy the j -dependence **becomes** weaker. The improvement in the calculations cannot be traced to a particular optical model parameter but presumably is a consequence of the fact that deuteron polarization measurements place a more rigid restraint on **all** parameters than cross section measurements alone. **Robson**²² has reported similar calculations for $^{40}\text{Ca}(d, p)$ using parameters which Satchler obtained by analyzing the Wisconsin polarization measurements. Robson expressed surprise about the failure of the earlier calculations because he **was** not aware that the inclusion of polarization measurements in the determination of the optical parameters was a **novel** feature. Robson's calculations on $^{54}\text{Fe}(d, p)^{55}\text{Fe}$ are based on optical model parameters which are incompatible with deuteron scattering from ^{54}Fe .

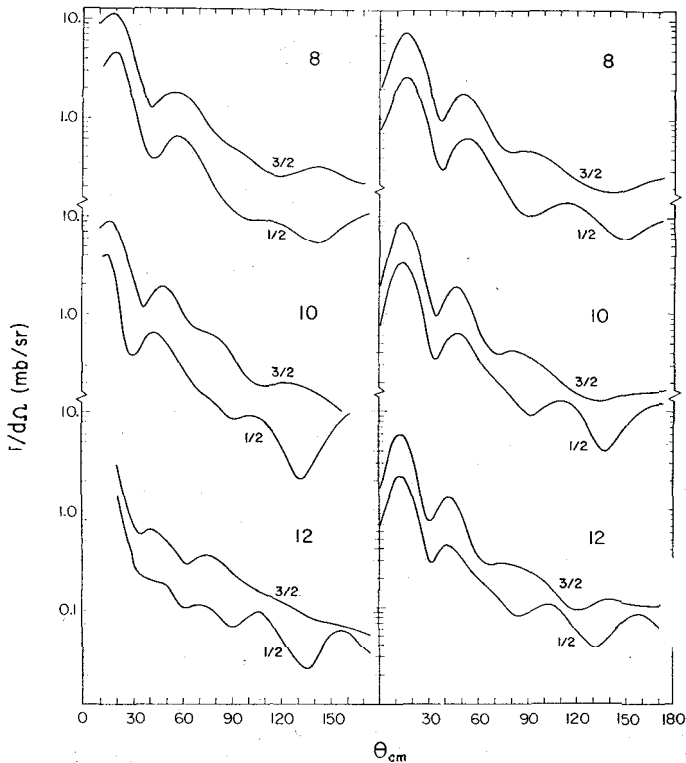
$^{54}\text{Fe}(d,p)^{55}\text{Fe}$ 

Fig. 13 - DWBA calculations of the $^{54}\text{Fe}(d,p)^{55}\text{Fe}$ cross sections at 8, 10 and 12 MeV (right-hand side of figure), compared to the measured cross sections (left-hand side). The calculations qualitatively reproduce the observed j -dependence.

We would expect that the spin-dependence of the deuteron potential should in some way be reflected in polarization effects in stripping reactions. One possible type of experiment is to measure the polarization of the outgoing nucleons in a double scattering experiment. If a polarized beam is available, however, it is much more convenient to measure the analyzing power. Yule²³ first showed that the analyzing power in stripping reactions is large and strongly spin-dependent. An example of recent results by Kocher is shown in Fig. 14. The curves were calculated without parameter adjustment from proton and deuteron optical potentials containing a

$^{52}\text{Cr}(d,p)^{53}\text{Cr}$ $E_d=10\text{MeV}$

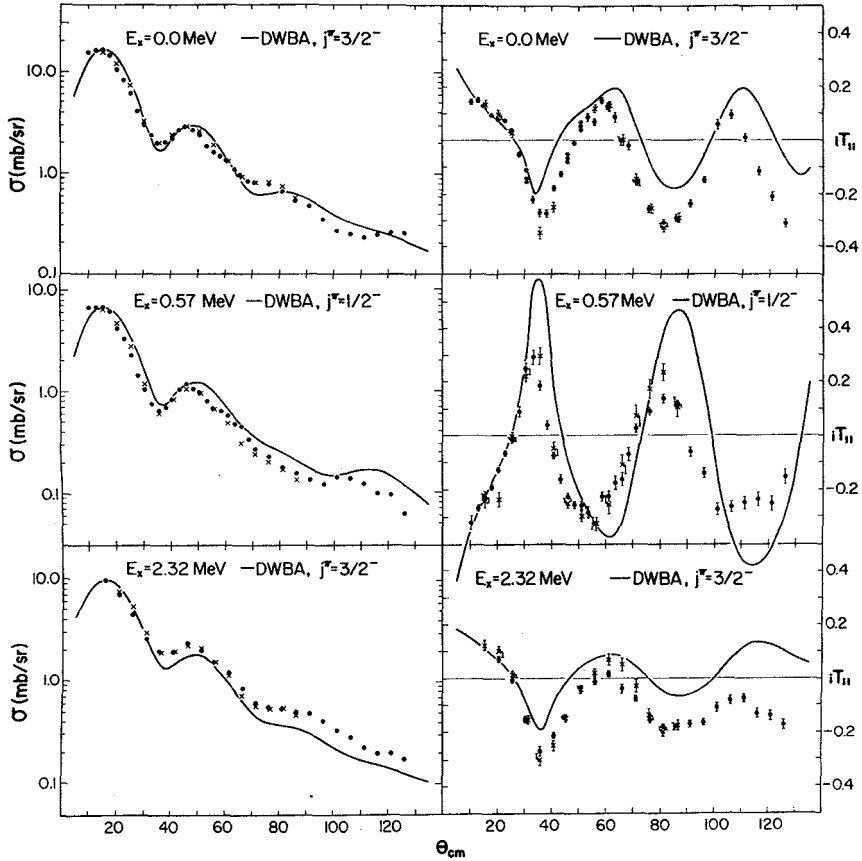


Fig. 14 - Differential cross sections and vector analysing powers of the reactions $^{52}\text{Cr}(d,p)^{53}\text{Cr}$.

spin-orbit term. However, results of this kind are not useful to test the correctness of the deuteron spin-orbit term since the analyzing power in fact arises primarily from the central distortions. This can be seen in Fig. 15 which shows calculations²³ of the analyzing powers for $^{40}\text{Ca}(d,p)^{41}\text{Ca}$ with and without spin-orbit terms in deuteron and proton potentials. For $^{28}\text{Si}(d,p)^{29}\text{Si}$ the spin-orbit term has a more pronounced effect, but experiments on this reaction indicate²⁴ that compound-nucleus formation contributes significantly to the reaction. The most promising approach is to study $l = 0$ transitions, because in this case the analyzing power an-

only through the spin-dependent distortions. Such measurements have been done on ^{88}Sr , ^{90}Zr , ^{117}Sn and ^{119}Sn and are found to be in reasonable agreement with DWBA calculations^{25,26}. It would be particularly interesting to compare (d, p)-analyzing powers with (d, p) polarization measurements since the proton and deuteron spin-orbit distortions enter in different ways and thus can be determined separately from one another. Instead of measuring the proton polarization, which is difficult experimentally, it is more advantageous to measure the analyzing power in the inverse (p, d)-reaction. Measurements of the analyzing powers in $^{119}\text{Sn}(d, p)^{120}\text{Sn}$ and in $^{120}\text{Sn}(p, d)^{119}\text{Sn}$ are now available²⁵ but unfortunately the two measurements are not at the same center-of-mass energy.

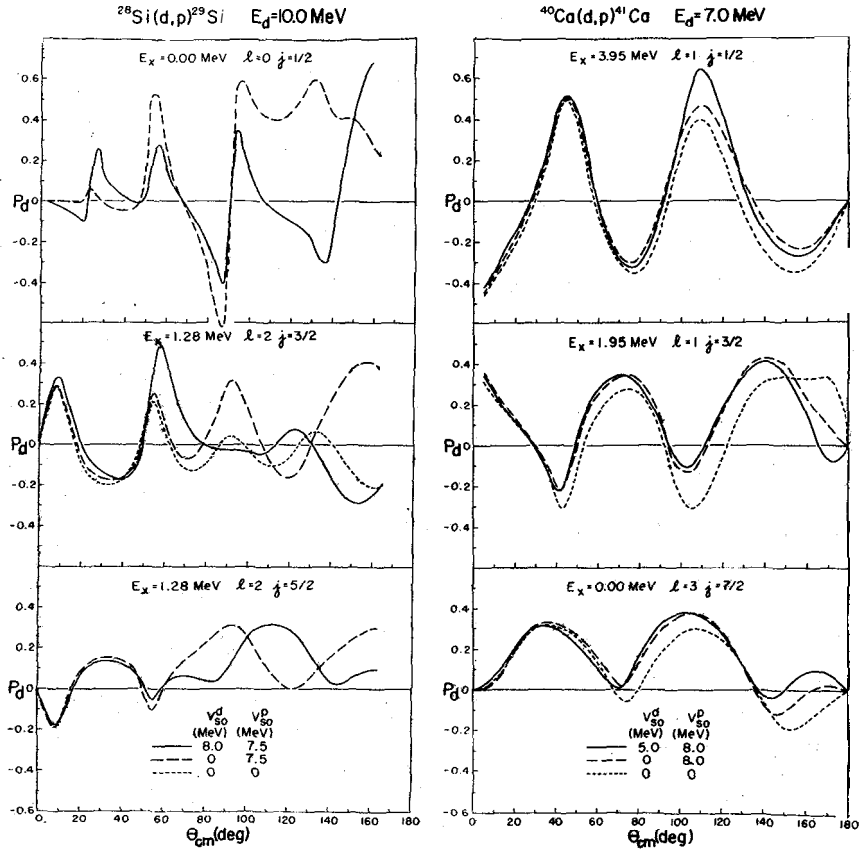


Fig. 15 - Calculated vector analysing powers of the reactions $^{28}\text{Si}(d, p)^{29}\text{Si}$ and $^{40}\text{Ca}(d, p)^{41}\text{Ca}$, for different strengths of the spin-orbit terms in the proton and deuteron potentials.

Another *interesting field* which is now *being explored* is the measurement of tensor analyzing powers in (d, p) -reactions. An example of very recent measurements by Rohrig is shown in Fig. 16. for the reaction $^{54}\text{Fe}(d, p)^{55}\text{Fe}$ at **10 MeV** bombarding energy. Particularly noteworthy is the fact that T_{21} is large, in contradiction to DWBA calculations using the potentials $V(\text{central}) + V(L \cdot S)$ derived from deuteron and proton elastic scattering. There is a **good chance** that we may learn more about the deuteron tensor interaction from such measurements.

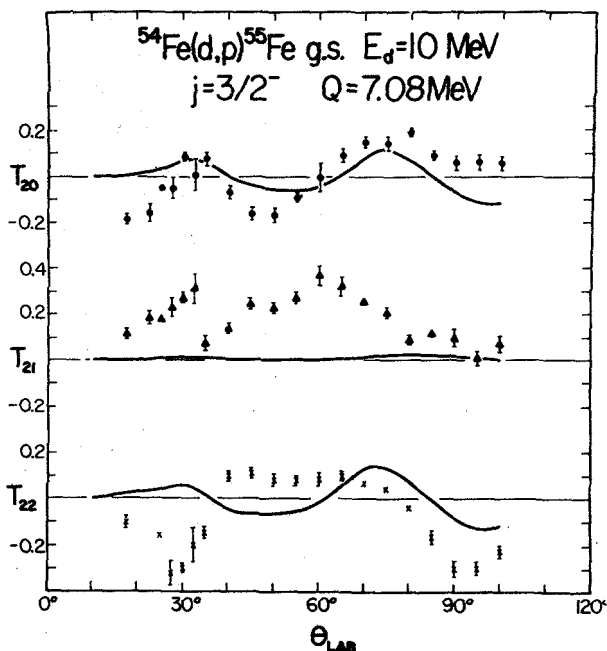


Fig. 16 - Tensor analyzing powers of the reaction $^{54}\text{Fe}(d, p)^{55}\text{Fe}$

7. Single Particle States

The spin-dependence of the deuteron-nucleus force can be seen in a particularly clear way in the scattering of deuterons from the α -particle. The most general way to analyze elastic scattering is to perform a phase-shift analysis. Because of the deuteron spin, for each value of l (except $l = 0$),

${}^4\text{He}(d,d){}^4\text{He}$

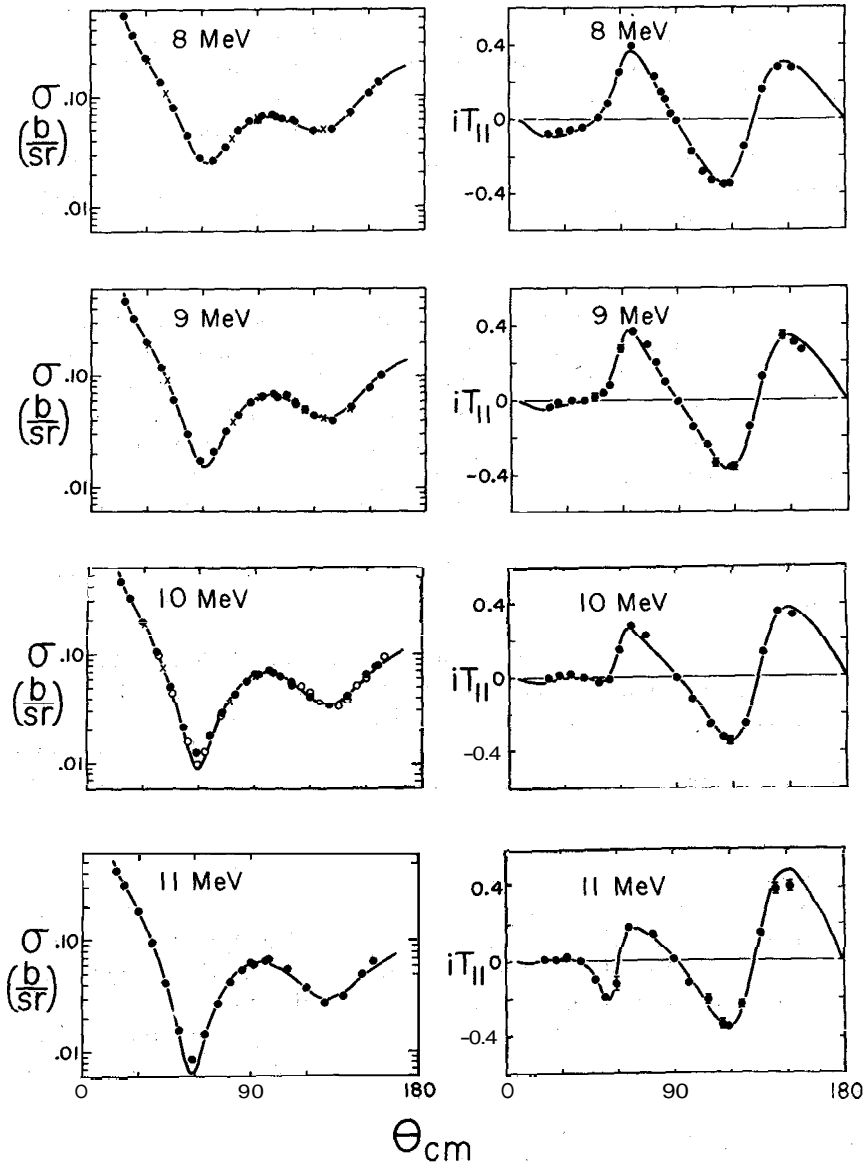


Fig. 17 - Differential cross sections and vector analysing powers of the elastic scattering of deuterons by ${}^4\text{He}$. The figure is from Ref. 30.

there will be three phase shifts corresponding to total angular momenta $J = l - 1, l$ and $l + 1$. Thus for $l \leq 2$, we are dealing with 7 complex phase shifts. If we make no simplifying assumption about the interaction, we must recognize the fact that tensor interactions, which do not conserve l , may be present. Off-diagonal elements are therefore introduced into the collision matrix which results in coupling of the s - and d -wave $J = 1$ phase shifts. The formalism for the inclusion of this coupling in a phase shift description of the scattering is given by Blatt and Biedenharn^{27, 28}. In the presence of such coupling the s - and d -wave $J = 1$ phase shifts are replaced by eigen phase shifts of the 2×2 $J = 1$ collision matrix plus a coupling parameter. These quantities are denoted by $\delta_\alpha, \delta_\beta$ and ϵ , respectively.

It is obviously not possible to determine the phase shifts uniquely from cross section measurements alone. The phase-shifts I am going to discuss were obtained by McIntyre several years ago²⁹ on the basis of crude (by present standards) measurements of all three tensor moments. Later, Keller³⁰ measured the vector analyzing power in d - α scattering and found that only minor adjustments in McIntyre's phase shifts were necessary to fit the data. A sample of his measurements and phase shift calculations is shown in Fig. 17. More recently, excellent measurements of the tensor analyzing power have been obtained at Zürich³¹ but again the (preliminary) analysis has shown qualitative agreement with the earlier results.

The main feature of the d - α phase shifts between 2 and 10 MeV is the absence of p -wave resonances and the presence of broad states of $J = 1^+$ and 2^+ . The energy dependence of the even-parity phase shifts is well reproduced by the single-level approximation of R -matrix theory. In Fig. 18, the solid curves show the phase shifts determined from experiment, the dashed lines are calculated from single-level theory. We see that the imaginary parts of the phase shifts are small. The unusual behavior of the $J = 1^+$ eigen phases $\delta_\alpha, \delta_\beta$ is explained by the assumption that the 1^+ -level has a large d -wave width ($\gamma^2 = 2.1$ MeV) and a small s -wave width ($\gamma^2 = 0.01$ MeV). The reduced width of the $J = 2^+$ resonance is also large ($\gamma^2 = 2.5$ MeV). Thus, we can think of both states as a deuteron with orbital angular momentum $l = 2$ moving in the field of the α -particle. This led us to try to describe d - α phase shifts by a simple potential well. A real potential was used since the imaginary parts of the phases are small. Obviously, we need a spin-orbit term to produce a splitting of the states with different J (2^+ and 1^+) but same l . Fig. 19 shows the experimental phase shifts (dots) compared to the potential model. Also shown is the low-energy region where there is a well-known $J = 3^+$ state near 1 MeV. The calculated curves show beautifully how the spin-orbit force splits the d -wave single

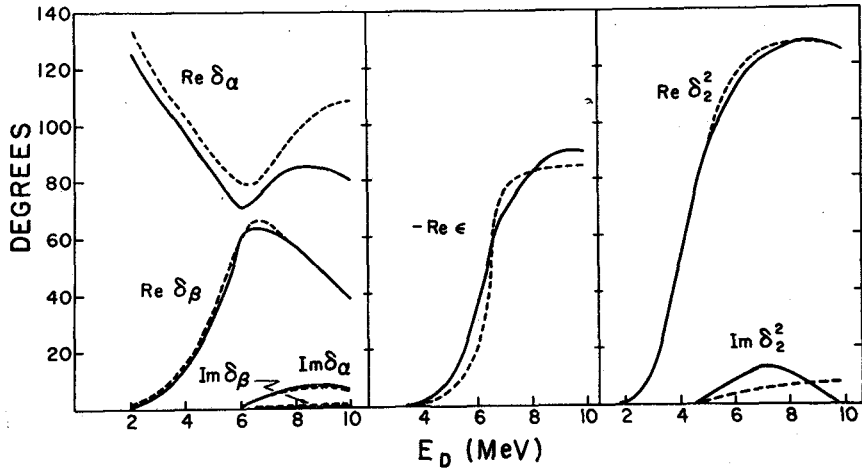


Fig. 18 - Calculated and experimental phase shifts for ${}^4\text{He}(d,d){}^4\text{He}$. The solid curves are from experimental data, while the dashed curves are based on single level theory. The figure is from Ref. 29.

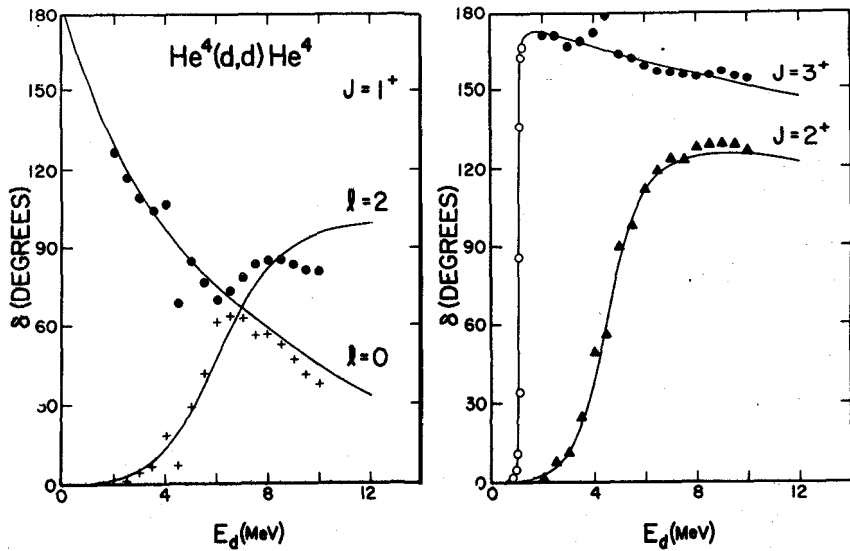


Fig 19 - Calculated and experimental phase shifts for ${}^4\text{He}(d,d){}^4\text{He}$. The dots are the experimental points and the curves are obtained from the potential model. The figure is from Ref. 29.

particle state into a triplet. The state of highest J is lowest in energy (“inverted triplet”) and also narrower than the others because the barrier (Coulomb and angular momentum) is larger for low energies. The calculation explains all features of the even-parity phase shifts, except those associated with the tensor interaction (non-crossing of eigen-phases). The calculated p -wave phase shifts are small ($< 20^\circ$), in qualitative agreement with the experimental phase shifts. The central potential used in the calculations was near **80 MeV**, instead of near **110 MeV** for the heavier nuclei discussed earlier, but this is offset by using a larger radius parameter (1.15 fm instead of **1.05**). Satchler *et al.*³² have shown that also p - α and n - α scattering is well described by a real optical potential.

8. Conclusions

The presence of a spin-orbit term in the deuteron optical model is clearly revealed from measurements of the vector analyzing power on many nuclei. A spin-orbit force of the Thomas form and geometrical parameters about **20%** smaller than those of the central potential gives an adequate description of the results. The spin-orbit strength is compatible with the Watanabe model but there are indications that agreement with the measurements can be obtained over a considerable range of values if all other parameters are readjusted. Accurate measurements of the total reaction cross section would be helpful.

Measurements of the tensor analyzing powers show that some form of tensor interaction is required. The effect of the tensor force is also seen in d - α scattering. From observations on Mg, Si, Al and Ca there is some evidence that the $\mathbf{S} \cdot \mathbf{r}$ tensor potential may be the most important one. The fact that two of the three forms of tensor interaction do not conserve l introduces a substantial complication in the calculations. The non-diagonal elements have been neglected in most calculations but this approximation must be studied further. The tensor effects caused by the quadrupole moment of the deuteron are found to be small.

The possibility to study the deuteron spin-dependence from polarization measurements on $l = 0$ stripping transitions has not yet been fully explored. Measurements are needed of the vector and tensor analyzing powers for (d, p) and the inverse (p, \mathcal{N}) reaction at the same center-of-mass energy. Recent measurements of the T_{21} analyzing power in stripping reactions suggest that this term is particularly sensitive to the deuteron tensor interaction.

I should like to thank my students **whose** work is **quoted in** this paper for **their** help and many stimulating discussions.

References and Notes

1. P. E. Hodgson, *Adv. in Physics* **15**, 329 (1966).
2. S. Watanabe, *Nucl. Phys.* **8**, 484 (1958).
3. S. Testoni and L. C. Gomes, *Nucl. Phys.* **89**, 288 (1966).
4. F. D. Becchetti, Jr. and G. W. Greenlees, *Phys. Rev.* **182**, 1190 (1960).
5. S. E. Darden, *Polarization Phenomena in Nuclear Reactions* (H. H. Barschall and W. Haerberli, Eds.), University of Wisconsin Press, 1971, p. 39.
6. B. L. Donnally, *Polarization Phenomena in Nuclear Reactions* (H. H. Barschall and W. Haerberli, Eds.), University of Wisconsin Press, 1971, p. 295.
7. H. F. Glavish, *Polarization Phenomena in Nuclear Reactions* (H. H. Barschall and W. Haerberli, Eds.), University of Wisconsin Press, 1971, p. 267.
8. P. Schwandt and W. Haerberli, *Nucl. Phys.* **A123**, 492 (1969).
9. R. Beurtey *et al.*, *Comp. Rend.* 256,922 (1963) and *Compt. Rend.* 257, 1477 (1963).
10. In Ref 3, the factor 2 on the right-hand side of Eq. (34) should be deleted.
11. J. A. R. Griffith, M. Irshad, O. Karban and S. Roman, *Nucl. Phys.* **A146**, 193 (1970).
12. J. Raynal, *Phys. Letters* **3**, 331 (1963) and *Phys. Letters* **7**, 281 (1964).
13. P. Schwandt and W. Haerberli, *Nucl. Phys.* **A110**, 585 (1968).
14. G. R. Satchler, *Nucl. Phys.* **21**, 116 (1960).
15. R. C. Johnson, *Polarization Phenomena in Nuclear Reactions* (H. H. Barschall and W. Haerberli, Eds.), University of Wisconsin Press, 1971, p. 143.
16. J. Raynal, *Polarization Phenomena in Nuclear Reactions* (H. H. Barschall and W. Haerberli, Eds.), University of Wisconsin Press, 1971, p. 153.
17. J. Raynal, Thesis, Paris 1964, unpublished.
18. A. Djalois and J. Nurzynski, to be published.
19. L. L. Lee, Jr. and J. P. Schiffer, *Phys. Rev. Letters* **12**, 108 (1964).
20. L. L. Lee, Jr. and J. P. Schiffer, *Phys. Rev.* **136**, B405 (1964).
21. C. Glashauser and M. E. Rickey, *Phys. Rev.* **154**, 1033 (1967).
22. B. A. Robson, *Physics Lett.* **26B**, 501 (1968).
23. T. J. Yule and W. Haerberli, *Nucl. Phys.* **A117**, 1 (1968).
24. D. C. Kocher, P. J. Bjorkholm and W. Haerberli, *Nucl. Phys.* **A172**, 663 (1971).
25. L. J. B. Goldfarb, *Polarization Phenomena in Nuclear Reactions* (H. H. Barschall and W. Haerberli, Eds.), University of Wisconsin Press, 1971, p. 205.
26. W. Haerberli, *Polarization Phenomena in Nuclear Reactions* (H. H. Barschall and W. Haerberli, Eds.), University of Wisconsin Press, 1971, p. 235.
27. J. M. Blatt and L. C. Biedenharn, *Revs. Mod. Phys.* **24**, 258 (1952).
28. J. M. Blatt and L. C. Biedenharn, *Phys. Rev.* **86**, 399 (1952).
29. L. C. McIntyre and W. Haerberli, *Nucl. Phys.* **91**, 382 (1967).
30. L. G. Keller and W. Haerberli, *Nucl. Phys.* **A156**, 465 (1970).
31. V. König, W. Grüebler, P. A. Schmelzbach and P. Marmier, *Polarization Phenomena in Nuclear Reactions* (H. H. Barschall and W. Haerberli, Eds.), University of Wisconsin Press, 1971, p. 588 and p. 590.
32. G. R. Satchler, L. W. Owen, A. J. Elwyn, G. L. Morgan, and R. L. Walter, *Nucl. Phys.* **A112**, 1 (1968).